

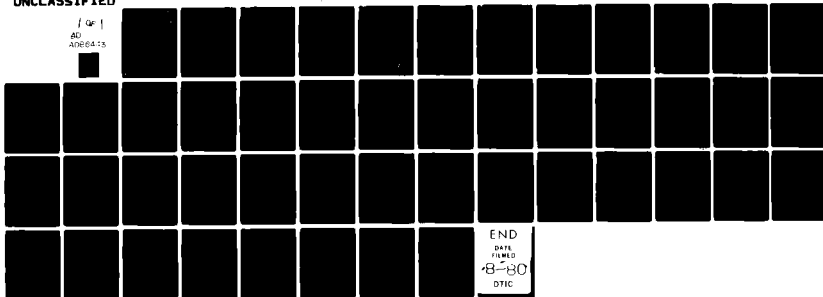
AD-A086 443

CALIFORNIA UNIV BERKELEY DEPT OF PHYSICS F/G 20/3
SUPERCONDUCTIVE DEVICES FOR MILLIMETER WAVE DETECTION MIXING AN--ETC(U)
1980 P L RICHARDS, T SHEN N00014-75-C-0496

NL

UNCLASSIFIED

1 QP 1
AD
A0864-13



END

DATE

FILED

8-80

DTIC

ADA 086443

LEVEL

11 1988

12

12 48

SUPERCONDUCTIVE DEVICES FOR MILLIMETER
WAVE DETECTION MIXING AND AMPLIFICATION

10 P. L./Richards T-M./Shen

DTIC
ELECTE
S JUL 3 1980 D

Department of Physics, University of California
Berkeley, California 94720

Contract N00014-75-C-0496

15

ABSTRACT

Single particle (quasiparticle) tunneling through an insulating barrier between two superconductors or between a superconductor and a normal conductor is being used to make very low noise detectors and mixers for millimeter wavelengths. The nonlinearity of the I-V curve obtained from tunneling between two superconductors can be so strong that classical theory breaks down and photon assisted tunneling theory must be used to understand device performance. Quantum theory predicts that a quasiparticle tunnel junction can be operated as a microwave photon detector with quantum efficiency close to unity or as a heterodyne mixer with conversion gain and with mixer noise temperature comparable with the quantum noise limit $T_M = \hbar\omega/k$. Both of these predictions have been experimentally realized at 36GHz using superconductor-insulator-superconductor junctions. It appears probable that these quasiparticle detectors and mixers will supercede the corresponding Josephson effect devices at millimeter wavelengths.

OMEGA

T. M.
DISTRIBUTION STATEMENT A
Approved for public release
Distribution Unlimited

071970

30 5 25 081

DDC FILE COPY

INTRODUCTION

Applications such as radio astronomy have stimulated development of low noise receivers for millimeter and submillimeter wavelength electromagnetic radiation. Heterodyne receivers are usually used for both line spectroscopy and for broad band radiometry at millimeter wavelengths. Direct detectors become competitive for broad band measurements at submillimeter wavelengths. Superconducting tunnel junctions have long been considered as possible nonlinear elements for low noise receivers in this wavelength range. The properties of Josephson effect detectors, mixers and parametric amplifiers have been investigated by many workers and are described in several review articles [1-3]. They have not been actively used, largely because the overall performance obtained has not kept ahead of the rapid development of cooled Schottky barrier diode mixers [4,5], InSb mixers [6] and composite bolometric detectors [7].

Detectors and mixers based on quasiparticle tunneling currents in superconducting junctions have developed rapidly in the past two years. Some of these devices now appear to be competitive for low noise applications. In this article we will review the recent progress in quasiparticle devices. For purposes of comparison, a brief summary will then be given of the present status of Josephson effect detectors, mixers, and parametric amplifiers.

The first type of quasiparticle junction to be used for detection and mixing experiments was the super-Schottky diode [8-11]. This is a superconductor-insulator-normal conductor (SIN) tunneling structure made with a superconducting Pb spot on a semiconducting substrate. The Schottky barrier created on the surface of the semiconductor provides the tunneling barrier. At temperatures less than the superconducting transition temperature T_c ,

thermionic emission over the barrier can be neglected and the diode current is dominated by quasiparticle tunneling. Superconductor-insulator-normal metal SIN junctions could also be used for quasiparticle devices, but have not been widely explored. More recent device work has made use of superconductor-insulating oxide-superconductor (SIS) devices fabricated by techniques similar to those described in this issue [12].

The metal-oxide technology used for SIS and SIN junctions is highly developed compared with the technology of the super-Schottky devices. In the former case there has been enormously greater investment, first for basic research, and then for digital Josephson effect devices. Reliable procedures exist for optical and electron beam lithography which can produce junctions with sub-micron dimensions. Large numbers of junctions, individual or in arrays, can be produced with uniform and predictable properties. Lifetime effects and effects of thermal cycling have been extensively studied and in many cases ways to control junction degradation have been devised. The availability of this junction technology is strongly influencing the present development of quasiparticle devices.

QUASIPARTICLE TUNNELING

Microwave effects have played an important role in the understanding of superconducting tunnel junctions. Historically the work of Dayem and Martin [13], which was interpreted as photon assisted quasiparticle tunneling by Tien and Gordon [14], was the first example of this line of inquiry. In Josephson's original paper [15], he theoretically explored the interaction of microwaves with the pair tunneling current. In both the quasiparticle tunneling and pair tunneling, the microwave signal frequency-modulates the wavefunctions and produces sidebands which appear as "steps" on the static I-V curve. The amplitude of the n th step is related to the Bessel function

$J_n(\alpha)$, where $\alpha = eV_1/\hbar\omega$ is a measure of the RF voltage V_1 . The step separation is $\hbar\omega/e$ for quasiparticle tunneling and $\hbar\omega/2e$ for Josephson tunneling. Despite these superficial similarities the details of the operation of quasiparticle devices are very different from those of Josephson devices.

The theory of quasiparticle tunneling has been studied extensively. In a recently published paper, Tucker [16] has given a complete review of those aspects of the theory which are relevant for detection and mixing. Rather than repeat this material we present here a simple qualitative discussion which is intended to assist the uninitiated reader to obtain an intuitive grasp of the physics involved.

In a superconductor the strong electron-phonon interaction causes a pairing of electrons near the fermi energy. These electron pairs are responsible for the lossless supercurrent in the bulk metal and the Josephson or pair current in superconductor-insulator-superconductor (SIS) tunnel junctions. The energy 2Δ required to break a pair is referred to as the superconducting energy gap. Sufficiently large thermal energies kT , photon energies $\hbar\omega$, or voltage drops eV (across tunneling structures) can break pairs and create single particle excitations called quasiparticles. The effective mass and density of states for quasiparticles near the fermi energy are very different from those for free electrons.

Tunneling of quasiparticles through an insulating barrier between two superconductors, or between a superconductor and a normal fermi sea, can be described in terms of the "semiconductor model." In this model each superconductor is represented by the density of quasiparticle states with an energy gap of width 2Δ at the fermi surface. In Fig. 1 we show the density of quasiparticle states plotted horizontally and energy plotted vertically for an SIN tunnel junction. A similar diagram for a superconductor-insulator-

PROPERTIES OF REAL JUNCTIONS

A number of phenomena occur in the junctions used for quasiparticle devices in addition to the idealized quasiparticle tunneling process described above. In order to understand the promise and the limitations of quasiparticle devices, these phenomena must be considered in some detail.

The properties of real SIN and SIS junctions can be discussed in terms of the equivalent circuits shown in Fig. 3. The quasiparticle tunneling current is represented by a nonlinear resistance which is shunted by the junction capacitance. In the case of SIN junction, there is a spreading resistance in series with the junction. In the case of SIS junctions, Josephson or pair tunneling provides a parallel conduction path which is represented by the symbol J . Series resistance is negligible in the SIS device at temperatures $T \ll T_c$. We will now discuss the properties of the nonlinear resistance, the series resistance, the junction capacitance and the Josephson current in real junctions.

The curvature parameter $S = (d^2I/dV^2)/(dI/dV)$, which appears in the classical analysis of detectors and mixers, can be used as the basis of comparison of the nonlinear resistance in different junctions. Nearly ideal super-Schottky junctions have been made with $S = e/kT = 7,700V^{-1}$ at 1.5K and $11,660V^{-1}$ at 1K over a significant voltage range [8-11]. The S parameter would be infinite for an ideal SIS device biased at the voltage $2\Delta/e$. In practice there is always some (essentially linear) leakage current through the junction and some rounding of the corner due to effects such as energy gap anisotropy, inhomogeneities in the metals and the insulator, and to strong coupling effects such as the quasiparticle lifetime. This rounding, which in many cases is independent of temperature, plays a critical role in the performance of SIS devices. Values of $\sim 10,000V^{-1}$ have been measured for

Pb-In-Au alloy junctions produced by the IBM sputter-oxidation technique [18]. Values of $22,000\text{V}^{-1}$ are obtained in sputter-oxidized Pb-Bi junctions [19]. Values in excess of $100,000\text{V}^{-1}$ have been observed in thermally oxidized Sn and Pb-alloy SIS junctions.

The series resistance present in SIN junctions produces parasitic losses as the junction capacitance charges and discharges through it twice each cycle. These parasitic losses limit the frequency response of present GaAs super-Schottky diodes to ~ 30 GHz. Higher frequency operation could probably be obtained by using a superconductor-insulating oxide-normal metal SIN structure. Since the SIS junction has negligible series resistance at low temperatures, its operation at mm-wavelengths is not hindered in this way.

In order for a junction to function as a nonlinear device at microwave frequencies, its capacitance must be small enough not to short out the microwave signal. This capacitance is proportioned to Ad^{-1} , where A is the junction area and d is the barrier thickness. The junction resistance R_N varies as $A^{-1}\exp(d)$. It will be argued that the best quasiparticle device performance is obtained when $R_N \sim X_C = (\omega C)^{-1}$. Consequently, the operating frequency ω varies as $d \cdot \exp(-d)$. Junctions with thin barriers, and thus with a small $R_N A$ product, are required for high frequency operation. A certain amount of capacitance at the signal frequency ω_s can be resonated out by the microwave imbedding network if the junction series resistance is not too large. Although the junction area plays no role in governing the frequency response of the device, there is a second requirement that the junction resistances should lie in a range which can be coupled to the input and the output. The input resistance R_{RF} and the output resistance R_{IF} of optimized devices are comparable to R_N . Either a single small junction

or a series array of larger junctions can be used to meet this matching condition.

The capacitance of several types of SIS junctions has been studied extensively. The results [20] are given in Fig. 4. Individual SIS junctions have been made with thin enough barriers and small enough areas to operate at frequencies well above 300GHz [21,22].

Josephson, or pair tunneling, provides a conductance path in SIS junctions that is not present in SIN junctions. In the absence of a magnetic field, SIS junctions will conduct a dc Josephson current up to a critical value I_c with no voltage drop. The value of I_c in an ideal junction at $T=0$ is equal to $\pi\Delta/2eR_N$ which is $\pi/4$ times height of the step in the quasiparticle current at $V=2\Delta/e$. When a finite voltage drop exists across an SIS junction there is an ac Josephson current,

$$I = I_c \sin\left[-\frac{2e}{h} \int^t V(t) dt\right], \quad (2)$$

When the current is increased from $I=0$, the junction voltage remains zero until I exceeds I_c . It then jumps to the quasiparticle curve at $V \approx 2\Delta/e$. If the capacitance is sufficiently large that $V(t)$ is essentially constant, then the sinusoidal Josephson current with frequency $\omega_J = 2eV/\hbar$ averages to zero and makes no contribution to the static I-V curve. The lower branch of the I-V curve, which is traced out as the current is decreased from a value above I_c , is essentially the quasiparticle tunneling curve in Fig. 2. The SIS quasiparticle devices are operated in this limit.

If the junction capacitance is compared with the normal resistance, the static I-V curve is then

currents (2) and, as illustrated in Fig. 5, the quasiparticle tunneling is not directly observed [23]. This low capacitance limit is reached with the point contact junctions that are used for Josephson effect detectors and mixers [1-3]. In the discussion of SIS quasiparticle devices that follows we assume that the capacitance is large enough to short circuit the junction at the Josephson frequency, and that the junction operating point remains on the quasiparticle branch of the I-V curve. Under these conditions the effects of Josephson tunneling on SIS device performance are small, and will be neglected. The effects of the Josephson current will be considered again in the discussions of Josephson effect mixers and parametric amplifiers.

PHOTON ASSISTED QUASIPARTICLE TUNNELING

Considered from a quantum-mechanical point of view, the junction current results from the tunneling of individual electrons from filled states on one side of the barrier into empty states of equal energy on the other. Taking one side as a reference, the electron wave functions have a time dependence of the usual form,

$$\phi_i(r,t) = \phi_i(r) \left\{ \exp \left[-\frac{i}{\hbar} \int^t E_i(t') dt' \right] \right\}. \quad (3)$$

In the presence of an applied potential $V + V_1 \cos \omega t$, the energy difference becomes

$$E_i(t) = E_i + e(V + V_1 \cos \omega t). \quad (4)$$

The usual Bessel series expansion can be used for this frequency-modulated wave function

$$\phi_i(r,t) = \phi_i(r) \sum_{n=-\infty}^{\infty} J_n(\alpha) \exp \left[-\frac{i}{\hbar} (E_i + eV + n\hbar\omega) t \right], \quad (5)$$

where $\alpha = eV_1/\hbar\omega$. The junction current can be calculated using a conventional

quantum mechanical prescription,

$$I^{QM}(t) = \sum_{m=-\infty}^{\infty} \sum_{n=-\infty}^{\infty} J_n(\alpha) J_{n+m}(\alpha) I(V + n\hbar\omega/e) e^{im\omega t}. \quad (6)$$

The low frequency junction current is obtained from (6) by setting $m=0$. In the presence of RF power, the static I-V curve has the form of a sum of the I-V curves observed without RF, each with amplitude given by $J_n^2(\alpha)$ and each displaced in voltage by the amount $n\hbar\omega/e$. The sharp onset of quasiparticle tunneling at the energy gap voltage in an SIS tunnel junction is thus reproduced over and over as a series of steps [14] as is shown in Fig. 6(a). The junction current (6) depends on the static I-V curve only at the bias point and at the "photon points" above and below the bias point shown in Fig. 6(b), which are separated by voltages equal to $\hbar\omega/e$. If the onset of quasiparticle tunneling is not sharp over the voltage range $\hbar\omega/e$, then the junction current is given by the classical limit of Eq. (6). The steps on the static I-V curve then wash out and the static current in the presence of RF power is simply the classical average of the instantaneous current over one complete RF cycle.

DIRECT DETECTION

The nonlinearity in the quasiparticle I-V curve can be used to produce very sensitive direct detectors or rectifiers at millimeter wavelengths. The classical expression for the current responsivity R_i of a small signal detector which is matched to the RF source can be written in the form

$$R_i^{CL} = \frac{(d^2I/dV^2)}{2(dI/dV)} = \frac{S}{2}, \quad (7)$$

where the derivatives are evaluated at the bias voltage. Because the S-values of conventional Schottky barrier diodes are small, microwave receivers which use such a direct detector at the front end are relatively noisy. Both

detector noise and amplifier noise prevent the detection of very small signals.

Because of their large S -values, however, quasiparticle junctions can be used to make very sensitive direct detectors. If the nonlinearity is strong enough that $S/2 > e/\hbar\omega$, then (7) is no longer valid. In the high frequency limit, the quantum analysis provided by Tucker and Millea for a tunneling device [16,24] must be used. The quantum expression for current responsivity obtained from (6) is

$$R_i^{QM} = \frac{e}{\hbar\omega} \left[\frac{I(V + \hbar\omega/e) - 2I(V) + I(V - \hbar\omega/e)}{I(V + \hbar\omega/e) - I(V - \hbar\omega/e)} \right]. \quad (8)$$

This result is similar to (7), except that the derivatives are replaced by finite differences. The responsivity in the small signal limit depends on the junction properties only at the bias point and at the two neighboring photon points as is illustrated in Fig. 6(b). If the knee on the I - V curve at the bias point is sharp enough that $I(V - \hbar\omega/e) \approx I(V) \ll I(V + \hbar\omega/e)$ then the current responsivity approaches the quantum limited value $e/\hbar\omega$. In this limit one electron crosses the junction for each photon absorbed. The theory then describes a microwave photon detector with unit responsive quantum efficiency.

In addition to the current responsivity, the RF resistance of the direct detector is modified by quantum effects. In the classical limit, this resistance is given by $R_{RF} = R_D = dV/dI$. The corresponding quantum expression again involves a finite difference,

$$R_{RF} = \frac{2\hbar\omega}{I(V + \hbar\omega/e) - I(V - \hbar\omega/e)}. \quad (9)$$

If the junction is not driven from a matched RF source, the responsivity will be reduced by the usual impedance mismatch factor $4R_{RF}R_S/(R_{RF}+R_S)^2$. Since the bias voltage is larger than $2kT/e$, shot noise in the bias current will

be observed in the detector [16,25],

$$i_N^2 = 2eI(V)B, \quad (10)$$

where B is the post-detection bandwidth. The theoretical noise-equivalent-power (NEP) for a matched diode can thus be written as

$$\text{NEP} = \langle i_N^2 \rangle^{1/2} / R_i^{\text{QM}} = (2eIB)^{1/2} / R_i^{\text{QM}}, \quad (11)$$

which approaches $\hbar\omega(2IB/e)^{1/2}$ in the quantum limit. An effective diode temperature T_D can be defined by equating i_N^2 from (10) to the thermal equilibrium noise from a device with dynamic resistance R_D . The value obtained $T_D = eIR_D/2k = e/2kS$ is equal to half the ambient temperature for an exponential device with $I = I_0 \exp[eV/kT]$. It can be even smaller for an SIS junction biased with $eV = 2\Delta$ because the S -value can be larger.

The limit to the detector NEP set by fluctuations in the input radiation power P in the bandwidth B_{Det} from a background temperature T_B is

$$\text{NEP} = (2PkT_B B_{\text{Det}} B)^{1/2}, \quad (12)$$

in the Raleigh-Jeans limit. Quasiparticle detectors have generally been evaluated under conditions in which $T_B \approx T$ and B_{Det} is small, so this contribution to the noise has been negligible.

Inverse frequency noise will adversely affect the performance of quasiparticle detectors in experiments which use low modulation frequencies. Experiments on SIS junctions suggest that the inverse frequency noise may extend well above 1kHz [26]. Detector measurements thus far have measured noise only in the 30-350MHz range.

The first quasiparticle detection experiments were done at 9GHz by the Aerospace group using super-Schottky (SIN) diodes in the classical limit [8-10]. Values of $R_i = 2,200 \text{ AW}^{-1}$ and $\text{NEP} = 5.4 \times 10^{-16} \text{ WHz}^{-1/2}$ were measured. Some loss was present which could be traced to the series spreading resistance. Subtracting this loss, the estimated performance would be $R_i = 5,500 \text{ AW}^{-1}$ and $\text{NEP} = 2.2 \times 10^{-16} \text{ WHz}^{-1/2}$. Very similar performance was obtained recently at 31GHz ($\text{NEP} = 4.8 \times 10^{-16} \text{ WHz}^{-1/2}$) [11]. It would appear difficult to obtain good performance at very much higher frequencies from the super-Schottky diode.

Detection experiments [27] have been reported in Pb-In-Au alloy SIS junctions [18] at 36GHz. The measured value of R_i was $3,500 \text{ AW}^{-1}$ which was half of the quantum limited value $e/h\omega$ and 0.79 of the value predicted from (8). This small discrepancy was ascribed to an RF impedance mismatch. The dependance of R_i on bias voltage was in good agreement with the quantum theory as is shown in Fig. 7. The measured NEP was $2.6 \times 10^{-16} \text{ WHz}^{-1/2}$ in excellent agreement with the shot noise theory (11). When corrected for impedance mismatch this value could be as low as $2.0 \times 10^{-16} \text{ WHz}^{-1/2}$. This SIS direct detector is a millimeter-wave photo-diode with a responsive quantum efficiency of 0.5. The detector noise arises from shot noise in the excess current near the full gap voltage which, for a given type of junction, tends to scale inversely with the impedance of the junction in the normal state. Hence, lower values of NEP are obtained by using higher impedance junctions. Other types of junctions with lower leakage current are well known. In particular, Sn or Pb alloy junctions fabricated using thermal oxidation techniques have very sharp corners on their I-V curves. If such junctions are used for direct detection, the reduced value of excess current could lower the NEP significantly. The sharper corner on the I-V curve would permit the limiting responsivity $R_i^{\text{QM}} = e/h\omega$ to be reached at frequencies below 36GHz.

Direct detectors are potentially useful for applications in which very large RF bandwidths are required. Depending on the operating frequency and the status of competing heterodyne devices, they may also be of value for radiometry (temperature measurement). The receiver noise temperature T_R of a heterodyne radiometer with a bandwidth B_{Het} which would give the same performance as the direct detector used with an input bandwidth B_{Det} is $T_R = NEP \sqrt{B_{Het}} / k B_{Det}$. Using the measured NEP of the SIS detector and practical values for the bandwidths $B_{Het} = 1\text{GHz}$ and $B_{Det} = 10\text{GHz}$, we obtain $T_R \approx 60\text{k}$. Both the bandwidth B_{Det} available to the direct detector and the quantum noise limit to the heterodyne receiver temperature T_R increase with frequency. Consequently, the direct detector becomes more competitive at high frequencies. Since the SIS junction has negligible series resistance at low temperatures, operation at submillimeter wavelengths appears to be feasible.

MIXING IN THE CLASSICAL LIMIT

Mixing experiments with quasiparticle junctions operated in the classical limit were first done with super-Schottky diodes [8-10] and then with SIS diodes [3, 28]. The ideal classical mixer is a switch which is opened and closed by each cycle of the local oscillator (LO). Quasiparticle mixers are dc biased near the knee at Δ/e (for SIN) or $2\Delta/e$ (for SIS). The instantaneous bias point is driven up and down the I-V curve by the LO. For voltages $V(t)$ below the knee R_D is large and the switch is open. For a range of values of $V(t)$ above the knee, R_D is small, so the switch is closed. If it were not for the onset of quantum effects, an SIS mixer with a sharp corner on the I-V curve would approach the ideal switch limit of mixer operation [29]. An important mixer parameter which is analogous to the responsivity of a detector is the conversion efficiency L^{-1} . It is defined as $L^{-1} = P_{IF}/P_S$, the ratio

of the available intermediate frequency power P_{IF} to the available signal power P_S . If the signal power is introduced equally into the sidebands above and below ω_{LO} , the double sideband (DSB) value of L^{-1} for a classical mixer can approach 1.0. If the signal appears only in one of the two sidebands, the signal is split between the two sidebands. If the two sidebands are terminated equally, the best possible (SSB) value of L^{-1} is 0.5. If the unused (image) sideband is mismatched, then L^{-1} (SSB) can approach 1.0. A classical resistive mixer cannot produce gain unless there is a region of negative resistance on the I-V curve [30].

The noise temperature of a microwave heterodyne receiver can be written as the sum of contributions from the mixer and from the intermediate frequency (IF) amplifier, $T_R = T_M + LT_{IF}$. There is a lower limit to mixer noise temperature $T_M \geq \hbar\omega/k$ set by quantum fluctuations which is 1.4K for $\lambda=1\text{cm}$ and 14K for $\lambda=1\text{mm}$. Since the noise temperature of cooled broadband transistor IF amplifiers is typically $T_{IF} \geq 10\text{K}$, the conversion efficiency plays an important role in limiting the achievable value of T_R at mm wavelengths.

The value of P_{LO} required for efficient operation of any of the superconducting mixers is a few μW compared with the mW power levels typically required to drive conventional Schottky diode mixers. This low power requirement is a result of the strong nonlinearity of both the Josephson and the quasiparticle diodes. It has significant advantages for the availability of LO sources, and the avoidance of both LO noise and LO heating of the small junction structures required at high frequencies. Because saturation effects are seen in a mixer when the signal power P_S reaches a small fraction of P_{LO} , low power operation is obtained at the cost of a reduction in the saturation level.

Several factors limit the amount of P_{LO} which can usefully be applied to a quasiparticle mixer. One limit arises from the saturation of the junction current at the value given by the normal state resistance R_N . A second limit in SIS devices arises from Josephson tunneling. If the instantaneous bias point passes through $V=0$, then Josephson effect steps will modify the I-V curve at the static bias point. Large conversion efficiency is seen under these conditions, but with such large noise as to render it of little practical value. It is believed that the mixing which occurs in this regime is closely related to the hysteretic Josephson effect mixing observed in point contact junctions [31]. These effects of pair tunneling can be reduced, but probably not eliminated by the application of a magnetic field.

The first quasiparticle mixing results were reported for a Pb-GaAs super-Schottky diode operated at 9GHz [8-10]. A SSB conversion efficiency $L^{-1} = 0.2$ and a very low SSB mixer noise temperature $T_M = 6K$ were observed. This noise corresponds to a diode temperature of $T_D = 1.2K$ at an ambient temperature of 1.06K. The corresponding performance at 31GHz [11] was $L^{-1} = 0.4$ and $T_M = 10K$, both SSB. As was the case for the direct detector, the diode spreading resistance caused some degradation of mixer performance and hinders extension of these results to higher frequencies.

Quasiparticle mixing in the classical limit has been investigated at 36GHz in SIS junctions [3, 28]. The SSB conversion efficiency was $L^{-1} = 0.22$ (after correction for impedance mismatch) and SSB mixer noise $T_M \leq 14K$ at an ambient temperature of 1.5K. This performance is comparable to that of the super-Schottky device, except that the absence of series resistance and the well developed junction technology make higher frequency operation promising. Some details of SIS mixer operation are given in Fig. 8. The

junction was an $\sim 9\mu\text{m}^2$ Pb-In-Au alloy device produced by the IBM sputter-oxidation procedure [18]. The normal resistance $R_N = 100\Omega$ was twice the reactance of the shunt capacitance at 36GHz. Part of this capacitance was resonated out by the microwave imbedding network.

The mixer signal in Fig. 8 shows two broad peaks which arise from the two regions of strong curvature on the static I-V curve. There is a null in the mixer output at a voltage which corresponds approximately to the point of inflection of the I-V curve. At this bias point the mixer, viewed as a switch, is turned off and on twice each cycle. There is no fundamental output ($\omega_S \approx \omega_{L0}$), but efficient harmonic mixing ($\omega_S \approx 2\omega_{L0}$) is expected. In one respect the mixer signal in Fig. 8(e) is not typical. It was measured with magnetic flux trapped in the junction which suppressed Josephson effects. Without this flux the mixer signal (e) and the cold RF load curve (d) (which is a measure of mixer noise) would both be much higher for bias voltages below $\sim 1.5\text{mV}$ where the $L0$ voltage swing includes the point at $V=0$. Both the super-Schottky and the SIS device performance were found to be in good agreement with classical 3-port Y-mixer theory. This theory includes the signal, the image, and the IF frequencies explicitly, but assumes that the capacitance is large enough to short circuit the junction at all harmonic frequencies.

In one important respect, the SIS mixer performance shown in Fig. 8 deviates from the expectations of classical theory. A series of small bumps separated in voltage by $\hbar\omega/e$ appear on the mixer signal which arise from photon assisted tunneling steps that are barely visible on the driven I-V curve. These quantum effects, which will be discussed in the next section, play a very important role in the performance of mixers made from junctions with sharper corners on their I-V curves.

QUANTUM THEORY OF SIS MIXERS

Evidence for quantum effects in the output of the first SIS mixers suggested that Tucker's full quantum formalism [16] should be used to compute the mixer performance expected from an SIS junction. At least three groups [32], including the authors, independently reached the surprising conclusion that conversion gain, that is, $L^{-1} > 1$ (DSB) was possible when the corner on the I-V curve is sharp enough compared with $\hbar\omega/e$ that quantum effects are strong. In order to fully explore the quantum effects, it was necessary to properly include the "real" as well as the "imaginary" part of the junction response function. This was first done by Tucker [33] who used both the real and the imaginary part of the theoretical SIS tunneling current [34] as the starting point for his calculation. Because of the inherent complexity of mixer theory, specific predictions are obtained only from a computer calculation. The simplest case of practical importance is the 3-port Y-mixer. As is the case with the theory of the direct detector, the mixer current in the presence of an RF drive has the general form given in (6). The junction response is of importance only at "photon points" separated by $\hbar\omega/e$. The theory does not depend on the shape of the I-V curve between photon points. The 3-port theory predicts conversion gain over a substantial range of terminating impedances. A region of arbitrarily large gain is found that is accompanied by negative dynamic resistance at the IF frequency. The "real" part of the junction response leads to quantum contributions to the mixer capacitance which are important only for operating frequencies which are comparable with the energy gap.

An analytic expression for conversion gain

$$L^{-1} = 2\Delta/\hbar\omega \quad (12)$$

has been obtained [35] from Tucker's formalism by expanding the Bessel functions in (6) in the limit in which the LO voltage V_1 is $\ll \hbar\omega/e$, but large compared to any rounding of the I-V curve.

The first measurements of mixer performance that were made with junctions whose I-V curves were sharp enough compared with $\hbar\omega/e$ to give significant quantum effects were done with Pb-In-Bi junctions at 115GHz [21]. These measurements were a part of a program to develop a practical receiver which has now been used successfully on a radio telescope [36]. They were done before the predictions of conversion gain were available. Mixer parameters of $L^{-1} = 0.2(\text{SSB})$ and $T_M \lesssim 80\text{K}(\text{SSB})$, were deduced from the overall performance of a receiver with a noise temperature of 470K. These numbers were very encouraging from the viewpoint of receiver development, but showed no sign of the subsequently predicted conversion gain.

The first mixer experiments to show conversion gain [37] were done at 36GHz with Pb-Bi junctions [19] whose I-V curves shown in Fig. 9(a) were only a factor ~ 2 sharper than those of the Pb-In-Au junctions shown in Fig. 8(a) that gave essentially classical results. They were sharp enough for weak photon assisted tunneling steps to appear on the driven I-V curve (b). The mixer signal (e) showed pronounced bumps separated in voltage by $\hbar\omega/e$. As with the essentially classical results in Fig. 8, the mixer signal goes to zero at $V = 3\text{mV}$. Below 2mV both the mixer signal (e) and the mixer output with a cold RF input load (d) are large due to Josephson effects. When the signal and the image frequency were terminated so that the conversion efficiency was the same in both sidebands, the mixer parameters, after careful correction for IF cable absorption and mismatch, were $L^{-1} = 0.70(\text{SSB})$ and $T_M \leq 3\text{K}(\text{SSB})$.

When the upper sideband (USB) was mismatched, some image rejection was obtained giving LSB $L^{-1} = 0.91$, $T_M \leq 5K$, and USB $L^{-1} = 0.51$, $T_M \leq 9K$.

A conversion efficiency of 0.70 (SSB) or 1.40 ± 0.14 (DSB) is larger than can be understood from classical theory. It is clear evidence for the predicted conversion gain. The onset of gain is very rapid. The small difference between the I-V curves of Figs. 8(a) and 9(a) leads to a factor 4.4 increase in conversion efficiency. The mixer noise temperature $T_M \approx 3K$ (SSB) or $1.5 \pm 2K$ (DSB) is indistinguishable from the fundamental photon noise limit $T_M = \hbar\omega/k$ ($\approx 1.7K$ at 36GHz). The availability of conversion gain from a photon noise limited mixer makes it appear possible that the performance of millimeter wave SIS heterodyne receivers will approach the photon noise limit. This level of performance has been approached only by maser amplifiers at lower frequencies and by infrared heterodyne receivers at $10.6\mu m$ where $\hbar\omega/k = 1,500K$.

THEORETICAL MODELING

The fit of the photon assisted tunneling theory to the mixer data just discussed has been examined in some detail to determine whether the predicted gain mechanism was in fact operative [37]. The input data for the model were a series of I-V curves like those in Fig. 8(a) and (b) but measured with a range of values of P_{LO} . The real part of the junction response was computed from the Kramers-Kronig transform of the static I-V curve measured with $P_{LO}=0$. The IF load resistance was known to be 50Ω . The RF source impedance was assumed to be the same at the signal, local oscillator and image frequencies, and was obtained by fitting the model to the I-V curves measured with P_{LO} applied [37]. The value obtained for the mixer illustrated in Fig. 9, when it was optimized for maximum conversion efficiency, was $Z_S = 14.1 + j1.4\Omega$. The junction capacitance, which was included in Z_S , had been resonated out by the imbedding network. The imaginary part of the imbedding impedance at the first harmonic

(72GHz) was also determined by this procedure. The value obtained $(j2\omega c)^{-1} = -j5\Omega$ was within a factor two of that expected from the junction capacitance estimated from Fig. 4.

The predictions of quantum 3-port Y-mixer theory with no free parameters are shown in Fig. 9. The calculated mixer signal as a function of bias voltage with constant RF source impedance shows the same oscillations that appear in the experimental data. The agreement with the experimental mixer output shown in Fig. 9 is very good where the experimental output is high and the calculated T_M is 1.4K compared with the measured $1.5 \pm 2K$. The theoretical conversion efficiency, however, diverges rapidly as the bias voltage approaches 3mV. This striking result is understood in terms of the rapidly increasing first harmonic content of the LO waveform as the bias is increased toward 3mV. In 3-port Y-mixer theory these harmonics are rigorously shorted, so they do not degrade the conversion efficiency. In the experiment, the junction capacitance is not completely effective in shorting the harmonics, so a significant fraction of the signal power is converted to harmonic frequencies. Preliminary calculations using the 5-port Y-mixer model showed that the divergence in the conversion efficiency calculated from the 3-port model was no longer obtained. The predictions of the 5-port model were within a factor two of the experimental conversion efficiency at all voltages. The largest source of discrepancy between theory and experiment appeared to arise from the assumption of the same imbedding impedance at the signal, local oscillator and image frequencies. Experimentally, the shape of the envelope of the oscillations in the mixer output was significantly affected when the waveguide matching structures were adjusted so as to produce image rejection [37].

The sensitivity of the conversion gain to the terminations at harmonic frequencies may be one reason that gain was not observed in the early mixer measurements at 115GHz [21].

Quantum mixer calculations were done to explore the usefulness of the SIS device as a harmonic mixer [38]. The strength of the quantum effects appears to depend primarily on the sharpness of the I-V curve compared with the size of the LO photon. Consequently, when the I-V curve in Fig. 9(a) was operated with $\nu_{LO} = 18\text{GHz}$ and $\nu_S = 36\text{GHz}$, essentially classical behavior was calculated with a conversion efficiency of $L^{-1} \approx 0.25$ and mixer noise $T_M \approx 30\text{K}$. Similar calculations with ν_{LO} at 60GHz and ν_S at 120GHz showed unlimited conversion gain with $T_M > 100\text{K}$. Even if it proves possible to operate in a region of small stable gain, the mixer noise will be greater than for the fundamental mixer. The noise arises from shot noise in the junction current which has a larger average value in the harmonic mixer because it is biased higher on the I-V curve. Despite this additional noise the SIS device has considerable promise as a first harmonic mixer. Because of the low P_{LO} requirement, injection of the LO should be much easier than for Schottky diode harmonic mixers.

It would be desirable to obtain a physical understanding of the gain mechanism in the photon assisted quasiparticle tunneling theory. Thus far it has not been possible to identify any direct analogies between these quasiparticle devices and other gain producing systems such as masers, parametric

amplifiers, etc. Some limited insight can be obtained from the analogy with the Josephson effect mixer [1-3]. The junction I-V curve changes as the amount of P_{LO} applied changes. In a sense the measurement of this change is a mixing experiment. When both a large LO current and a small signal current are driven through a mixer diode, the net current is amplitude and phase modulated at the IF frequency. Neglecting the small phase modulation, the low frequency (IF) output is the same as for a weakly amplitude modulated LO source. When I-V curves are measured with slightly different values of P_{LO} , one can evaluate the derivative $(\partial I / \partial \sqrt{P_{LO}})_V$ which is a measure of the change in the static current for a given change in RF current. Since the static I-V curves are measured with a high impedance load, the junction dynamic resistance at low frequencies also appears in the power conversion efficiency,

$$L^{-1} = \left(\frac{\partial I}{\partial \sqrt{P_{LO}}} \right)^2 R_D. \quad (13)$$

The two factors in (12) were calculated using 3-port Y-mixer theory and the I-V curve in Fig. 9(a) in order to judge their relative importance in producing gain. It was found that in this particular case most of the gain arose from R_D which is the inverse of the derivative of the I-V curve with LO power applied. Unlimited gain is obtained from the theory when the photon assisted tunneling steps are sufficiently sharp that R_D becomes negative. Thus, the SIS mixer gain bears the same relationship to the steps on the driven I-V curve as does the gain in the Josephson effect mixer [31].

ARRAYS OF SIS JUNCTIONS

There can in principle be advantages in the use of series arrays of SIS junctions for mixing. The junction properties illustrated in Fig. 4 show that high operating frequencies can be achieved only if the Josephson critical current density J_c is large so that the product of area times normal

resistance $AR_N = \pi\Delta/2eJ_c$ is low. Techniques have been demonstrated that produce junctions small enough that convenient values of RF and IF impedance can be obtained in single junctions, even for frequencies well beyond 300GHz [21,22]. In particular cases, however, these techniques may not be available, or may not be compatible with other junction requirements such as power dissipation or sharpness of the I-V curve. The possibility exists of using a series array of n large junctions with area nA in place of a single smaller junction with area A . If the junctions are identical, the voltages scale is multiplied by a factor n so that the peaks in the mixer output are separated in voltage by $n\hbar\omega/e$. This behavior is illustrated in Fig. 10, which shows mixer output data for a series array of S_n junctions with $n=50$ [39]. The required P_{LO} is also increased by the factor n . This increase is unlikely to be a serious disadvantage for $n \lesssim 100$. The proportionate increase in mixer saturation power may be of value in some experiments. In practice, difficulties can be encountered with arrays of junctions that are not sufficiently uniform. Of necessity, each junction in an array is current biased at all frequencies. The static and LO bias voltages for a given junction will thus be directly related to its impedance. It is possible to have many of the junctions in the array biased far enough from $2\Delta/e$ that they provide no useful nonlinearity.

The best SIS array mixing results were reported using 40-junction arrays of Pb junctions in the classical limit at 9GHz [40]. Conversion efficiencies of $L^{-1} = 0.26$ and mixer noise in the range $T_M = 10-40K$ were observed. These results are sufficiently good to suggest that arrays of junctions may play a useful role in future quasiparticle mixers.

Series arrays of junctions are not as attractive for direct detection as they are for mixing. The effective S-value for an array of n junctions in series is S/n . In the classical limit, therefore, the current responsivity

of an n -junction array would be degraded by a factor n . The responsivity for an array whose individual junctions have S -values larger than the quantum limit $2e/\hbar\omega$ is given by $R_j = e/n\hbar\omega$, so is also degraded by the factor n .

Because of the importance of series resistance, a different use of arrays may be of value for super-Schottky devices. Parallel arrays of super-Schottky diodes have been fabricated to reduce the spreading resistance and thus permit operation at higher frequencies [41].

JOSEPHSON EFFECT MIXER

The capacitance of the SIS (Josephson) junctions discussed thus far in this review has been large enough that the ac Josephson oscillations at the instantaneous bias point, which is $2\Delta/e$ for an SIS mixer, are effectively shorted and do not contribute to the static junction current. In low-capacitance junctions with $C\hbar/2eR_N\Delta$, by contrast, the junction voltage can vary with time at the Josephson frequency and its harmonics. As is illustrated in Fig. 5, the time average of the Josephson current given by (2) then contributes significantly to the "quasiparticle" branch of the junction I-V curve [21]. Very low capacitance junctions can sometimes be adequately represented as having a linear resistance R_N at all voltages, rather than the non-linear quasiparticle tunneling characteristic of Fig. 2. This resistively shunted junction (RSJ) model is especially useful for point contacts or thin metallic bridges where the nonlinearity of the quasiparticle current can be significantly smeared or entirely absent.

In Fig. 11 we show static I-V curves with and without P_{LO} for a Nb point contact Josephson junction at 36GHz [31] whose response closely resembles the predictions of the RSJ model. The steps on the driven I-V curve arise from dc beats between the ac Josephson current and harmonics of the LO current. In the small signal limit $I_{RF} \ll I_C$, the static current decreases as I_{RF}^2 . Consequently, if no local oscillator power is applied, the junction will act as a square-law detector [1-3]. Theoretical estimates of

NEP for this device give results which are similar at millimeter wavelengths to the measured performance of the SIS direct detector. The best measured performance was $\text{NEP} \approx 3 \text{ and } 5 \times 10^{-15} \text{ WHz}^{-1/2}$ at 90 and 120 GHz. This NEP is expected to increase as ω_S^2 at higher frequencies, compared with the more favorable ω_S dependence for the SIS detector.

When sufficient P_{LO} is applied that $I_{RF} \approx I_C/2$, then the zero voltage current is significantly reduced and Josephson steps appear as is shown in Fig. 11(b). In this mode of operation, the static junction current decreases linearly with I_{RF} . The analysis which leads to (12) can be used to show that this device is a linear mixer which can have conversion gain at points of large dynamic resistance on the driven I-V curve.

The general principles of operation of the Josephson effect mixer have been well reviewed [1,3] so will not be discussed in detail here. Mixer performance, including noise, has been carefully analyzed using analog simulations [42] and digital [43] calculations. When a realistic model of the microwave imbedding network is included, the mixer noise T_M is significantly larger than either $\hbar\omega/k$, or the ambient temperature T_A . The cause of this noise is the efficient harmonic mixing displayed by the Josephson effect mixer. Broad-band noise in the mixer at RF frequencies, whether thermal or photon in origin, is mixed down into the IF band by beating with many harmonics of the LO frequency and with the ac Josephson frequency. A detailed treatment of these effects is given in the paper by Taur in this issue [43].

Careful experimental evaluation of Josephson effect mixers has been carried out at many frequencies. The results of these tests shown in Table I appear to confirm the theoretical prediction that the noise spectral density in the IF band is significantly larger than the noise in the signal band.

It is possible to make a number of comments about the comparison between Josephson effect and quasiparticle detectors and mixers. The Josephson devices

require very low capacitance junctions. Although progress is being made in the fabrication of evaporated film structures with the required properties [47, 48] all successful low noise detection and mixing experiments to date have used Nb point contact junctions. Despite much effort [44, 49] these junctions remain much less stable and reliable than the quasiparticle junctions. The Josephson effect mixer can be saturated by room temperature thermal noise, even for relatively modest coupling bandwidths [42]. This effect does not appear to be troublesome in the quasiparticle mixers [37]. The noise in the Josephson mixer appears to be significantly larger than that in quasiparticle mixers.

These comparisons so favor the quasiparticle devices, especially those from which gain can be obtained, that current development efforts are being strongly focused in this direction. Although this emphasis is probably justified, it should be kept in mind that relatively little is known about the performance of SIS mixers at frequencies above 36GHz.

JOSEPHSON EFFECT PARAMETRIC AMPLIFIERS

When an SIS junction is biased at zero voltage, it appears as a nonlinear RF inductance with a shunt resistance. It has been possible to use junctions biased in this way as the nonlinear element in externally pumped parametric amplifiers [2,3]. Parametric amplifiers pumped by the ac Josephson oscillations can also be made, but the noise is expected to be somewhat larger [2].

The externally pumped devices are being actively developed.

In the four-photon doubly degenerate amplifier developed by Chiao and co-workers [50], two pump photons at ω_p are used to produce a signal photon at ω_s and an idler photon ω_i such that $\omega_s + \omega_i = 2\omega_p$ and $\omega_s \approx \omega_i \approx \omega_p$. No dc bias is applied so the junction symmetry cancels parasitic oscillations at even harmonics of ω_p . In the three-photon singly degenerate amplifier developed by the Copenhagen group [51], a dc bias current $<I_c$ is applied to break the junction symmetry and a single pump photon splits into a signal photon and an idler photon such that

$$\omega_p = \omega_S + \omega_I \text{ and } \omega_S \approx \omega_I.$$

It has been possible to operate these devices using either thin film superconducting micro-bridges [50], point contact junctions [52], or evaporated film tunnel junctions [53]. In the first two cases the junction current is clamped by the series reactance. In the last case the junction voltage is clamped by the junction capacitance. In each instance the average value of the Josephson inductance and the internal junction capacitance (or an externally supplied capacitance) are in resonance at the signal frequency. Linear arrays of junctions have proved useful to provide the required RF impedance over a finite bandwidth. A large amount of detailed experimental and theoretical effort has contributed to the present understanding of these interesting devices [50-58]. The paper by Levinsen et al. in this issue [55] summarizes a unified description of both types of amplifiers.

It was initially hoped that Josephson effect parametric amplifiers would provide the front-end for photon noise limited millimeter wave receivers. This was a reasonable expectation because thermal or shot noise gives a contribution to the noise temperature of a properly terminated parametric amplifier which is comparable to the ambient temperature. This hope has not been realized because of the appearance of an unexpected noise phenomenon which is often referred to as the "noise rise." The dominant contribution to the amplifier noise temperature is observed to be proportional to its gain [52, 53, 56, 57]. It has recently been suggested that phase instability will be amplified in this way [55]. The operating point of a parametric amplifier executes a limit cycle which is phase-locked to the pump. If the convergence of the limit cycle is not sufficiently rapid, small amounts of phase noise are amplified to produce gain-dependent noise in the output. It has been suggested that this may be a property of any parametric amplifier [57].

Understanding of the noise rise phenomenon is critical for the future of Josephson effect parametric amplifiers. Only if this noise can be significantly reduced can these amplifiers be competitive with SIS mixer receivers. This question is under investigation, but a clear answer is not yet available.

A portion of this research was supported by the U.S. Office of Naval Research.

Table I. Experimental parameters of Josephson effect mixers made with Nb point contact junctions. The mixer noise is shown directly and also normalized to T_{eff} which is the larger of the ambient temperature or $\hbar\omega/k$.

Frequency [GHz]	SSB Conversion efficiency L^{-1}	SSB Mixer Noise Temperature $T_M(K)$	$\frac{T_M}{T_{\text{eff}}}$	Reference
36	1.4	54	33	[31]
115	1.0	120	18	[44]
135	0.3	180	34	[45]
450	0.3	350	16	[46]

Fig. 1. Densities of states $D(\epsilon)$ for SIN and SIS tunnel junctions (with the same superconductor on each side) in the neighborhood of the fermi energy ϵ_F . The energy 2Δ required to break a pair of electrons is shown as a gap in the densities of quasiparticle states for the superconductors. The normal conductor is represented by a constant $D(\epsilon)$. States which are filled at $T=0$ are shaded.

Fig. 2. Theoretical tunneling currents for SIN and SIS junctions calculated using Eq.(1) and the densities of states from Fig. 1.

Fig. 3. Equivalent circuits for SIN and SIS tunnel junctions.

Fig. 4 Nominal junction cut-off frequency $(2\pi R_N C)^{-1}$ plotted as a function of Josephson critical current density J for Pb tunnel junctions [20]. Junctions with $J_c > 10^5 \text{ Acm}^{-2}$ have been reported [21, 22].

Fig. 5. Effect of capacitance on the I-V curve of an SIS junction [23] when the junction cut-off frequency $(R_N C)^{-1}$ is high compared with the gap frequency, the time average of the nonsinusoidal ac Josephson current contributes significantly to the I-V curve at finite voltages. When $(R_N C)^{-1}$ is small, the quasiparticle current dominates the I-V curve at finite voltages. The calculations are not complete at low voltages.

Fig. 6(a). The appearance of photon assisted quasiparticle tunneling steps when a microwave signal is applied [14]. Steps are seen for the tunneling of a quasiparticle accompanied by the absorption of 4, 3, 2, 1 and zero photons and with the emission of one photon.

(b) The quantum theory for the current in a junction with static bias voltage V and microwave bias at frequency ω depends on the shape of the I - V curve at V and at photon points separated from it by $\hbar\omega/e$. The dashed lines are chords which illustrate the calculation of the current responsivity of a direct detector biased at the photon point indicated by the solid point. The current responsivity R_i^Q is proportional to the difference in the slopes of the chords a and b divided by the slope of the chord c .

Fig. 7(a). Measured I - V curve of a Pb(In, Au) alloy SIS tunnel junction at 1.4K. (b) Measured and calculated responsivities of the above junction operated as a direct detector. The experimental curve was measured with a constant RF source resistance which was close to optimum at the peak of the responsivity curve. The theoretical curves were computed for a constant RF source resistance, which was chosen in each case to minimize the rms deviations between the theory and the experiment. Although the differences between the classical and the quantum predictions are not generally large for these experimental parameters, the latter theory does provide a significantly better overall fit. One important aspect of the quantum theory is that it averages out the effects of features on the I - V curve which are narrow compared with $\hbar\omega/e = 0.15$ mV. For example the classical theory predicts a sharp (negative) peak in responsivity at a bias of 2.25 mV where there is a sharp kink in the I - V curve. This peak is not present in the quantum prediction and is not observed experimentally [27].

Fig. 8. Static I - V curves measured for a 1.5K Pb-In-Au junction (a) without and (b) with P_{LO} . Plots of IF amplifier output voltage in the frequency range from 30 to 80MHz are shown as a function of junction bias voltage. Curve (c) was obtained with a 50 Ω 1.5K load in place of the mixer; curve (d) with a matched 1.5K load in front of the mixer; curve (e) with a calibrated 36GHz signal applied to the mixer from a klystron oscillator. Values of mixer noise temperature were deduced from (c) and (d), and conversion efficiency from (e) [28].

Fig. 9. Static I-V curves measured for a Pb(29 wt. % Bi) junction at 1.5K (a) without P_{LO} and (b) with P_{LO} . Plots of IF output power in the frequency range from 30-80 MHz are shown as a function of junction bias voltage. Point (c) was obtained with a 50 Ω 1.5K load in place of the mixer, curve (d) with a matched 1.5K load in front of the mixer and curve (e) with a calibrated 36GHz signal applied to the mixer from an oscillator. Values of mixer noise temperature were deduced from (c) and (d), and conversion efficiency from (e). Curve (f) shows the oscillations in the mixer output calculated from quantum 3-port Y-mixer theory with no free parameters. Below 2.1 mV Josephson (pair tunneling) currents degrade mixer performance. In this region the mixer has high conversion efficiency, but also large noise [37].

Fig. 10(a). I-V curves with and without P_{LO} for a series array of $n=50$ S_n junctions. (b). Mixer output for this array showing photon assisted tunneling peaks separated by $50 \hbar\omega/e$ [39].

Fig. 11(a). I-V curve of a Nb point contact junction which is similar to the prediction of the RSJ model with zero capacitance. The load line used for the direct detector is indicated. (b) The same junction with sufficient P_{LO} to reduce the zero voltage current to $I_c/2$. The load line used for the heterodyne mixer is indicated. (c) Mixer output as a function of bias voltage showing peaks at voltages where R_D is large [31].

References 1

- [1] P. L. Richards, "The Josephson junction as a detector of microwave and far infrared radiation," Semiconductors and Semimetals, vol. 12, R. K. Willardson and A. C. Beer, Eds., New York: Academic, 1977, pp. 395-439.
- [2] R. Adde and G. Vernet, "High frequency properties and applications of Josephson junctions from microwaves to far infrared," Superconductor Applications: SQUIDS and Machines, B. B. Schwartz and S. Foner, Eds., New York: Plenum, 1976 - pp. 248-320.
- [3] P. L. Richards, "Millimeter wave superconducting devices," in Future Trends in Superconductive Electronics, B. S. Deaver, Jr. et al., Eds., New York: AIP Conf. Proc. 44, 1978 - pp. 223-229.
- [4] S. Weinreb and A. R. Keer, "Cryogenic cooling of mixers for millimeter and centimeter wavelengths," IEEE J. Solid State Circuits, vol. SC-8 - pp. 58-63, Feb. 1973.
- [5] R. A. Linke, M. V. Schneider, and A. Y. Cho "Cryogenic millimeter wave receivers using molecular beam epitaxy diodes," IEEE Trans. Microwave Theory Tech., vol. MTT-26, pp. 935-938.
- [6] T. G. Phillips and K. B. Jefferts, "A low temperature bolometer heterodyne receiver for millimeter wave astronomy," Rev. Sci. Inst., vol. 44, pp. 1009-1014, August 1973.
- [7] N. S. Nishioka, D. P. Woody, and P. L. Richards, "Composite bolometers for submillimeter wavelengths," Appl. Opt., vol. 17 - pp. 1562-1567, May 1978.
- [8] M. McColl, M. F. Millea, and A. H. Silver, "The superconductor-semiconductor Schottky barrier diode detector," Appl. Phys. Lett., vol. 23 - pp. 263-264, September 1973.
- [9] F. L. Vernon, Jr., M. F. Millea, M. F. Bottjer, A. H. Silver, R. J. Pederson, and M. McColl, "The super-Schottky diode," IEEE Trans. Microwave Theory Tech., vol. MTT-25 - pp. 286-294, April 1977.
- [10] M. McColl, M. F. Millea, A. H. Silver, M. F. Bottjer, R. J. Pederson and F. L. Vernon, Jr., "The super-Schottky microwave mixer," IEEE Trans. Magn., vol. MAG-13 - pp. 221-227, January 1977.
- [11] R. J. Pedersen, M. McColl, and A. H. Silver (to be published).
- [12] This issue.
- [13] A. H. Dayem and R. J. Martin, "Quantum interaction of microwave radiation with tunneling between superconductors," Phys. Rev. Lett., vol. 8 - pp. 246-248, March 1962.

References 2

- [14] P. K. Tien and J. P. Gordon, "Multiphoton process observed in the interaction of microwave fields with the tunneling between superconductor films," Phys. Rev., vol. 129 - pp. 647-651, January 1963.
- [15] B. D. Josephson, "Possible new effects in superconductive tunneling," Phys. Lett., vol. 1 - pp. 251-253, July 1962
 _____, "Supercurrents through barriers," Adv. Phys., vol. 14 - pp. 419-451, October 1965.
- [16] J. R. Tucker, "Quantum limited detection in tunnel junction mixers," IEEE J. Quantum Elect., vol. QE-15 - pp. 1234-1258, November 1979.
- [17] I. Giavar and K. Megerle, "Study of superconductors by electron tunneling," Phys. Rev., vol. 122 - pp. 1101-1111, May 1961.
- [18] R. A. Havemann, C. A. Hamilton, and R. E. Harris, "Photolithographic fabrication of lead alloy Josephson junctions," J. Vac. Sci. Technol., vol. 15 - pp. 392-395, Mar./April 1978.
- [19] J. H. Greiner, C. J. Kircher and I. Ames, "Fabricating process for Josephson integrated circuits," IBM J. Res. Devel., March 1980 (to be published).
- [20] R. E. Harris and C. A. Hamilton, "Fast superconducting instruments," Future Trends in Superconductive Electronics, B. S. Deaver, Jr. et al., Eds., New York: AIP Conf. Proc. 44, 1978 - pp. 448-458.
- [21] G. J. Dolan, T. G. Phillips, and D. P. Woody, "Low noise 115GHz mixing in superconducting oxide barrier tunnel junctions," Appl. Phys. Lett., vol. 34 - pp. 347-349, March 1979.
- [22] R. E. Howard, E. L. Hu, L. D. Jackel, L. A. Fetter, and R. H. Bosworth, "Small area high current density Josephson junctions," Appl. Phys. Lett., vol. 35 - pp. 879-881, December 1979.
- [23] D. G. McDonald, G. G. Johnson, and R. E. Harris, "Modeling Josephson junctions," Phys. Rev., vol. B 13 - pp. 1028-1031, February 1976.
- [24] J. R. Tucker and M. F. Millea, "Photon detection in nonlinear tunneling devices," Appl. Phys. Lett., vol. 33 - pp. 611-613, October 1978.
- [25] D. Rogovin and D. J. Scalapine, "Fluctuation phenomena in tunnel junctions," Annals of Physics, vol. 86 - pp. 1-90, July 1974.
- [26] J. Clarke and G. Hawkins "Flicker (1/f) noise in Josephson tunnel junctions," Phys. Rev., vol. B 14 - pp. 2826-2831, October 1976.
- [27] P. L. Richards, T-M Shen, R. E. Harris, and F. L. Lloyd, "SIS Quasiparticle junctions as microwave photon detectors," Appl. Phys. Lett., vol. 36 - pp. 480-482, March 1980.

References 3

- [28] P. L. Richards, T. M. Shen, R. E. Harris, and F. L. Lloyd, "Quasiparticle heterodyne mixing in SIS tunnel junctions," Appl. Phys. Lett., vol. 34 - pp. 345-347, May, 1979.
- [29] A. A. M. Saleh, Theory of Resistive Mixers, M.I.T. Press, Cambridge, Massachusetts, 1971.
- [30] H. C. Torrey and C. A. Whitmer, Crystal Rectifiers, M.I.T. Rad. Lab. Series, vol. 15, McGraw Hill, 1948.
- [31] Y. Taur, J. H. Claassen, and P. L. Richards, "Conversion gain in a Josephson effect mixer," Appl. Phys. Lett., vol. 24 - pp. 101-103, January, 1974.
- [32] T-M. Shen and P. L. Richards, J. R. Tucker and G. Solner (private communication).
- [33] J. R. Tucker, "Predicted conversion gain in superconductor-insulator-superconductor quasiparticle mixers," Appl. Phys. Lett., vol. 36 - pp. 477-479, March 1980.
- [34] N. R. Werthamer, "Nonlinear self-coupling of Josephson radiation in superconducting tunnel junctions," Phys. Rev., vol. 147 - pp. 255-263, July, 1966.
- [35] D. P. Woody and G. Solner (private communication).
- [36] D. P. Woody and T. G. Phillips (private communication).
- [37] T-M. Shen, P. L. Richards, R. E. Harris and F. L. Lloyd, "Conversion gain in mm-wave quasiparticle heterodyne mixers," Appl. Phys. Lett., (to be published), May, 1980.
- [38] T-M. Shen and P. L. Richards (unpublished).
- [39] T-M. Shen, P. L. Richards, R. Y. Chiao and M. J. Feldman (unpublished).
- [40] S. Rudner and T. Claeson, "Analysis of superconducting tunnel junctions as low-noise 10GHz mixers," Appl. Phys. Lett., vol. 34 - pp. 711-713, May, 1979.
- [41] M. McColl, M. F. Bottjer, A. B. Chase, R. J. Pedersen, A. H. Silver, and J. R. Tucker, "The super-Schottky diode at 30GHz," IEEE Trans. Magn., vol. MAG-15 - pp. 468-470, January 1979.
- [42] J. H. Claassen and P. L. Richards, "Performance limits of a Josephson junction mixer," J. Appl. Phys., vol. 49 - pp. 4117-4129, July 1978.
- [43] Y. Taur, "Josephson junction mixer analysis using frequency-conversion and noise correlation matrices," (this issue).
- [44] Y. Taur and A. R. Kerr, "Low-noise Josephson mixers at 45GHz using recyclable point contacts," Appl. Phys. Lett., vol. 32 - pp. 775-777, June 1978.

References 4

- [45] J. H. Claassen and P. L. Richards, "Point-contact Josephson mixers at 130GHz," J. Appl. Phys., vol. 49 - pp. 4130-4140, July 1978.
- [46] T. G. Blaney, "Josephson mixers at submillimeter wavelengths: Present experimental status and future developments," Future Trends in Superconductive Electronics, B. S. Deaver, Jr. et al., Eds. New York: AIP Conf. Proc. 44, 1978 - pp. 230-238.
- [47] M. Octavio, W. J. Skocpol, and M. Tinkham, "Nonequilibrium enhanced supercurrents in short superconducting weak links," Phys. Rev., vol. B17 - pp. 159-169, January 1977.
- [48] J. H. Claassen, "Josephson behavior in granular NbN weak links," (to be published).
- [49] M. J. Feldman, P. T. Parrish, and R. Y. Chiao, "Operation of the Superamp at 33GHz," J. Appl. Phys., vol. 47 - pp. 2639-2644, June 1976.
- [50] N. F. Pedersen, M. R. Samuelson, and K. Saermark, "Parametric excitation of plasma oscillations in Josephson junctions," J. Appl. Phys., vol. 44 - pp. 5120-5124, November 1973.
- [51] Y. Taur and P. L. Richards, "Parametric amplification and oscillation at 36GHz using a point contact Josephson junction," J. Appl. Phys., vol. 48 - pp. 1321-1326, March 1977.
- [52] S. Wahlsten, S. Rudner, and T. Claeson, "Arrays of Josephson tunnel junctions as parametric amplifiers," J. Appl. Phys., vol. 49 - pp. 4248-4263, July 1978.
- [53] O. H. Soerensen, B. Dueholm, J. Mygind, and N. F. Pedersen, "Theory of the singly quasi-degenerate Josephson junction parametric amplifier," J. Appl. Phys. (to be published).
- [54] M. T. Levinsen, N. F. Pedersen, O. H. Soerensen, B. Dueholm, and J. Mygind, "Externally pumped millimeter wave Josephson junction parametric amplifier," (this issue).
- [55] R. Y. Chiao, M. J. Feldman, D. W. Peterson, B. A. Tucker and M. T. Levinson, "Phase instability noise in Josephson junctions," Future Trends in Superconductive Electronics, B. S. Deaver, Jr. et al., Eds. New York: AIP Conf. Proc. 44, 1978 - pp. 259-263.
- [56] J. Mygind, N. F. Pedersen, O. H. Sorensen, B. Dueholm, and M. T. Levinson, "Low noise parametric amplification at 35 GHz in a single Josephson tunnel junction," Appl. Phys. Lett., vol. 35 - pp. 91-93, July 1979.
- [57] M. F. Feldman and M. T. Levinson, "Gain dependent noise temperature of Josephson parametric amplifiers," (to be published).

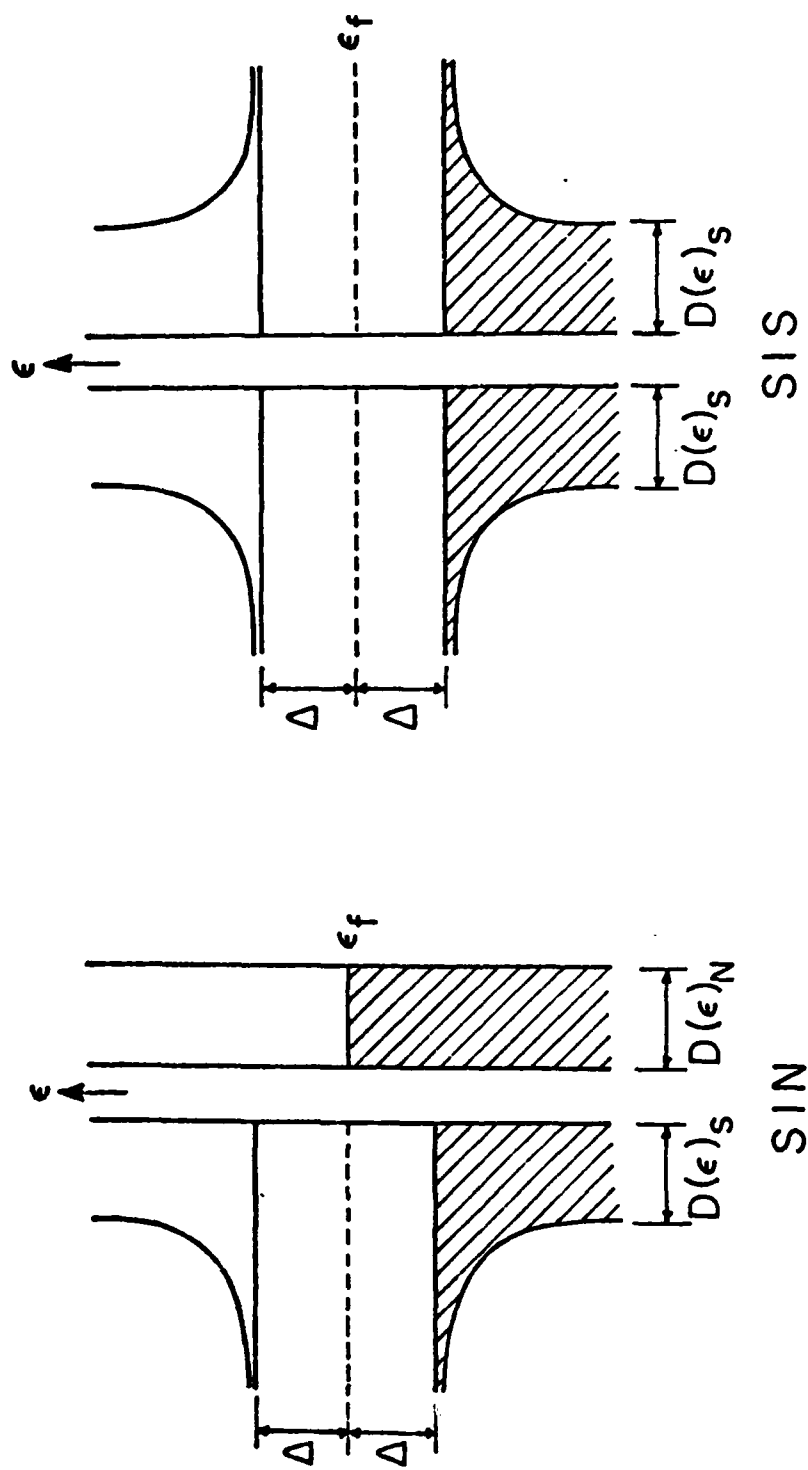


Figure 1.

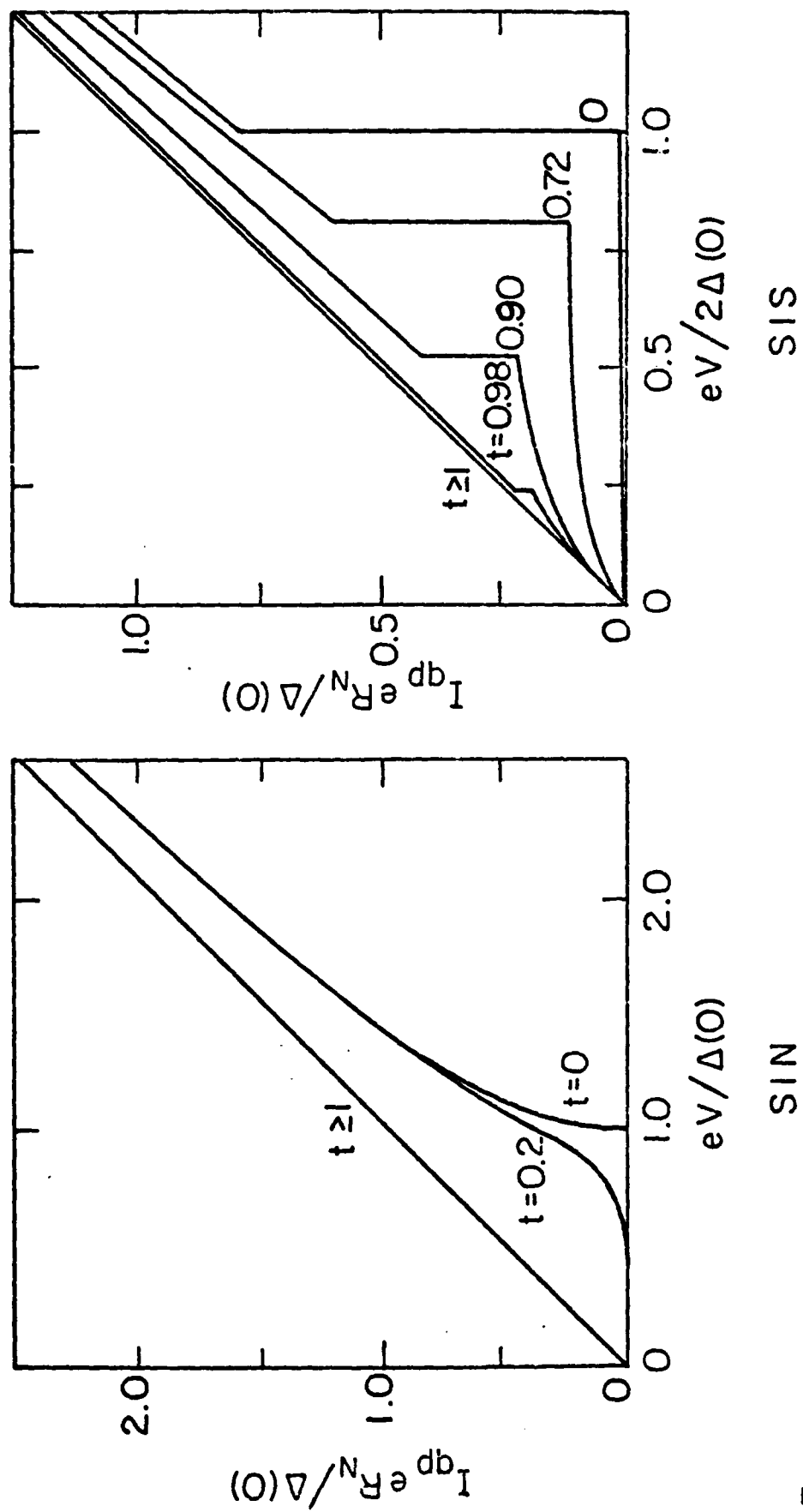
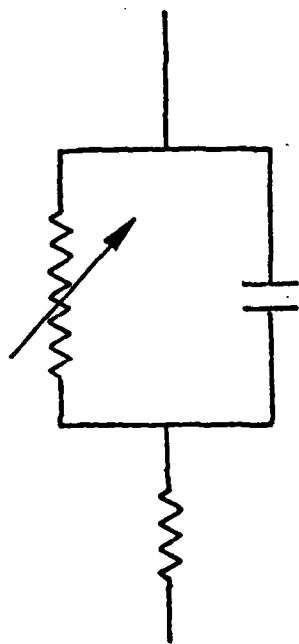
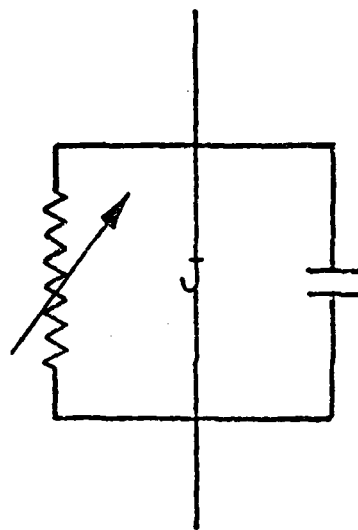


Figure 2.



SIN



SIS

Figure 3.

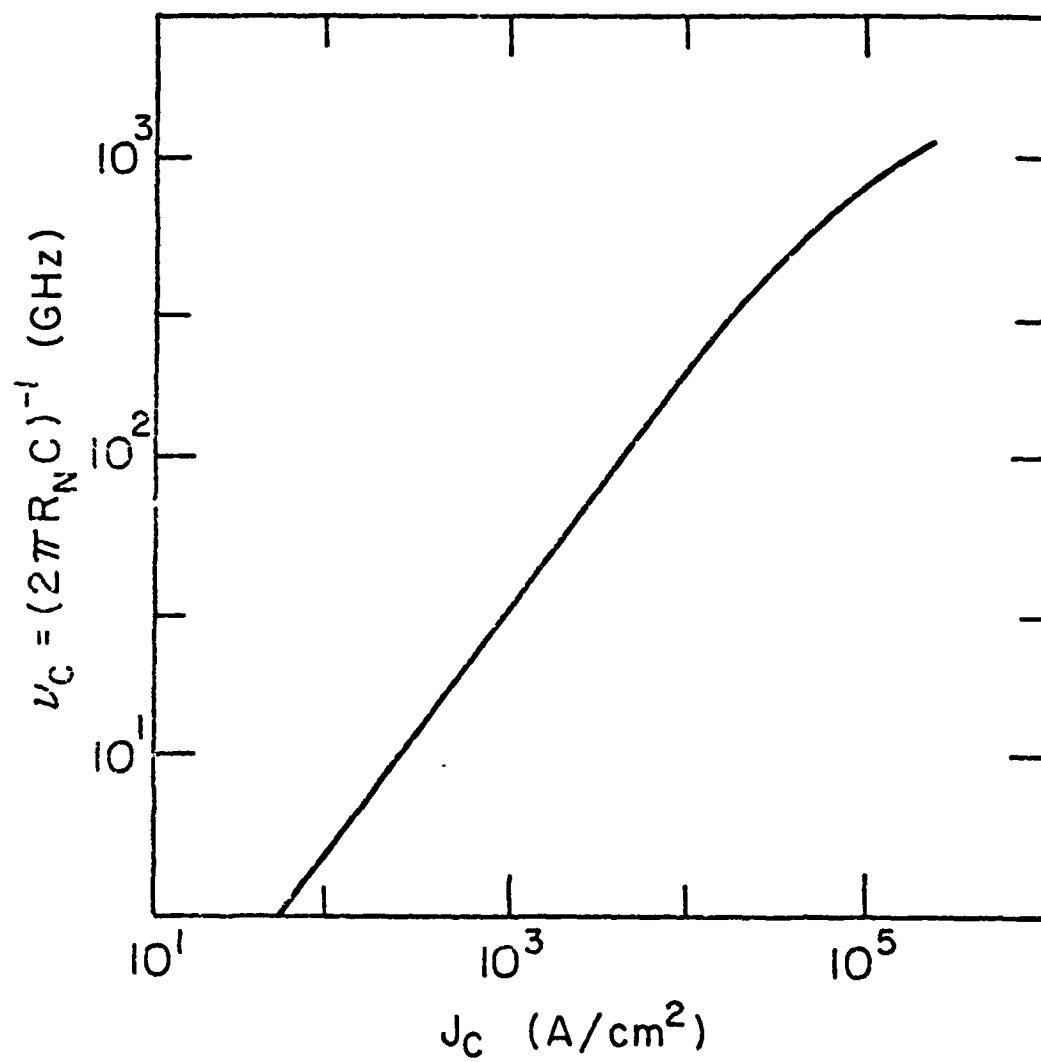


Figure 4.

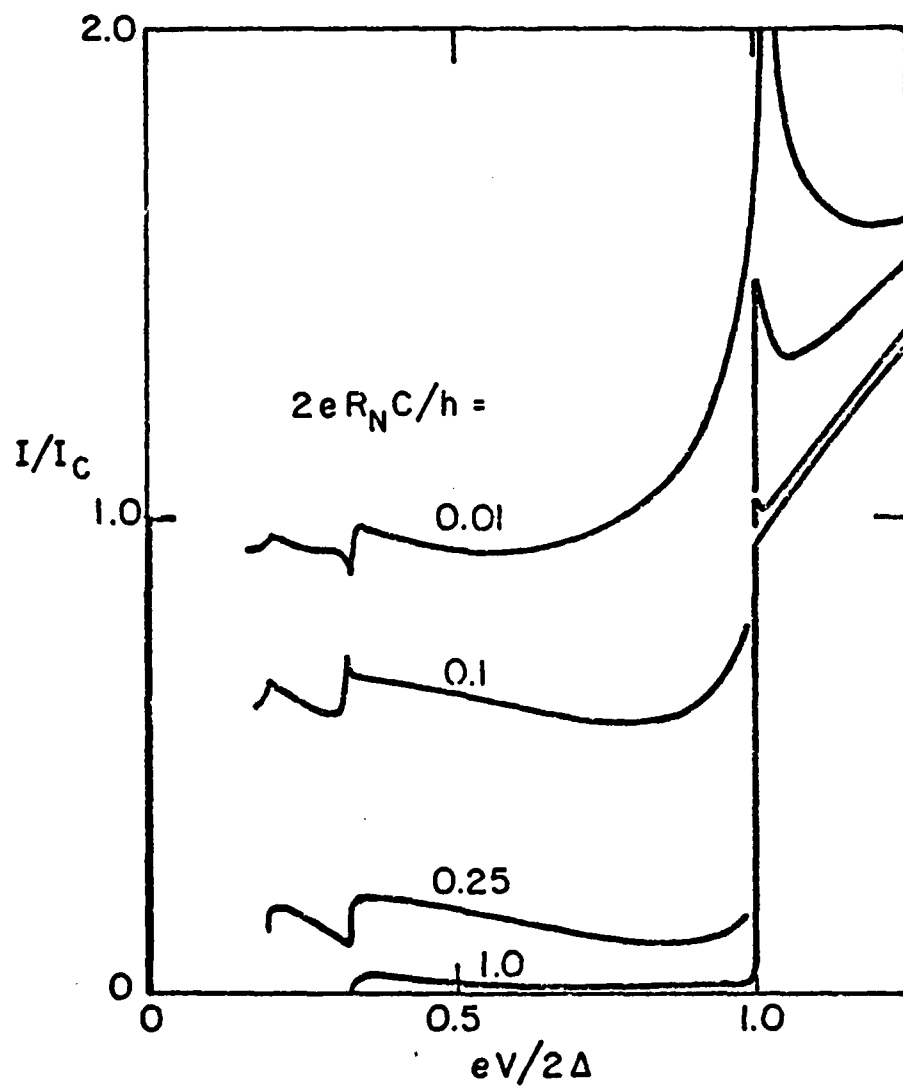


Figure 5.

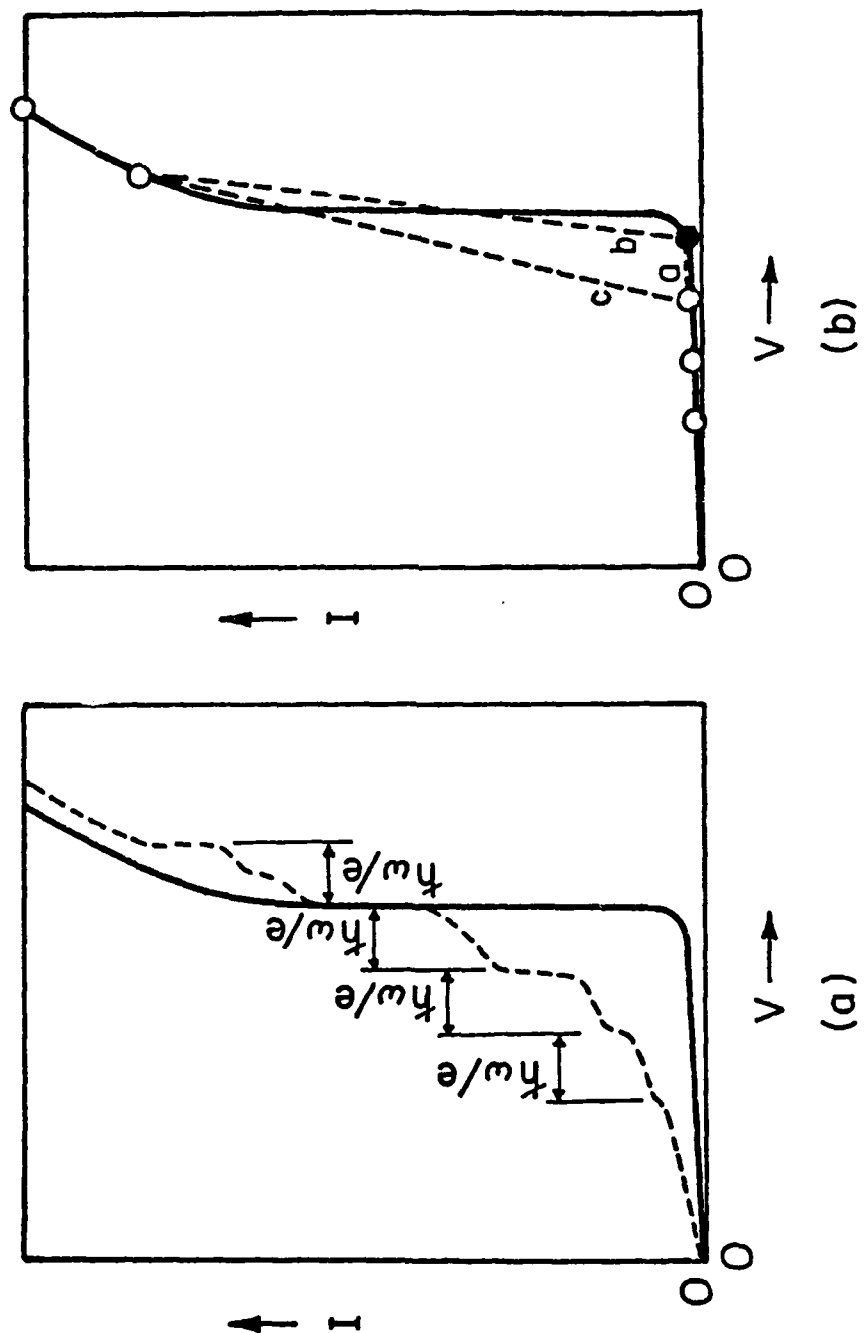


Figure 6.

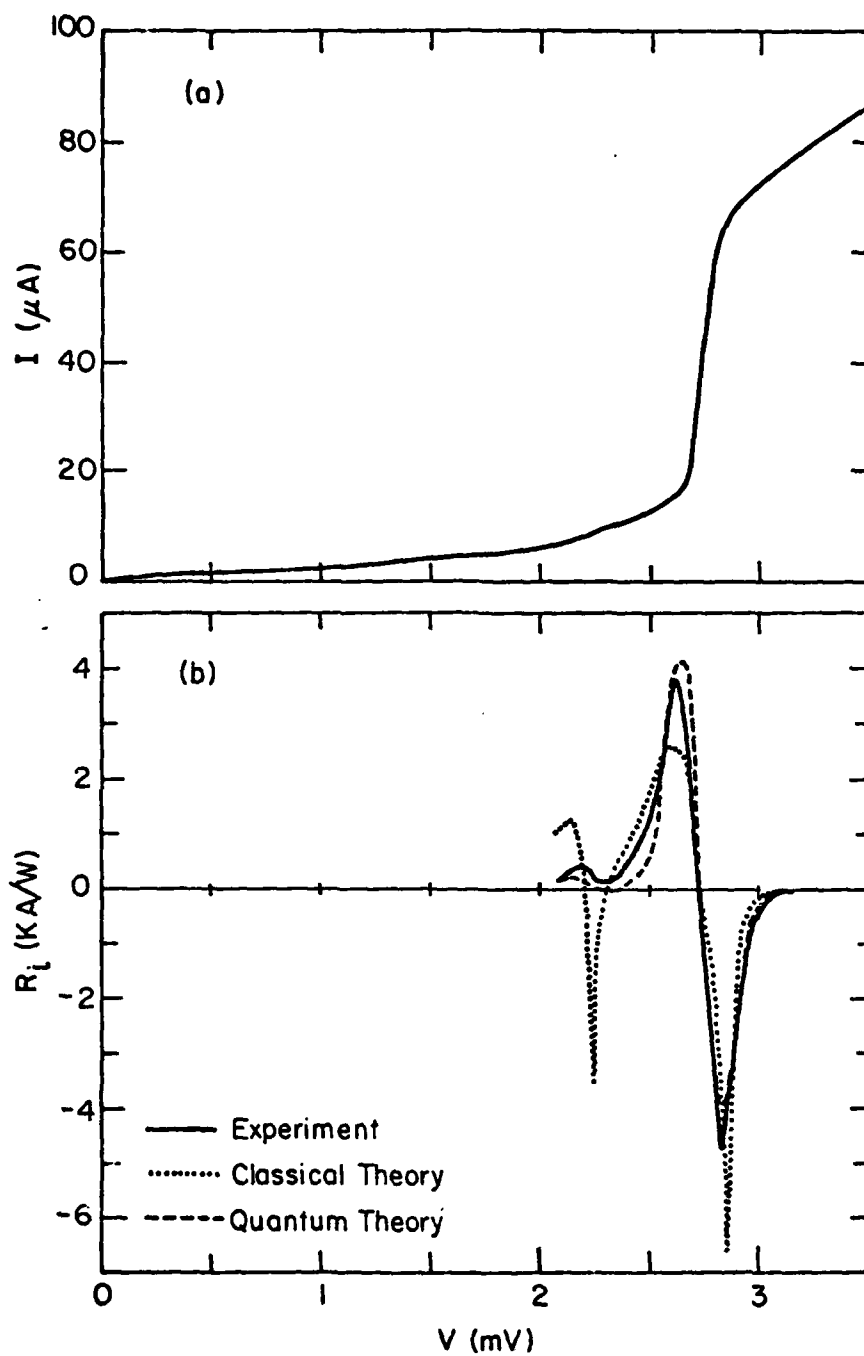


Figure 7.

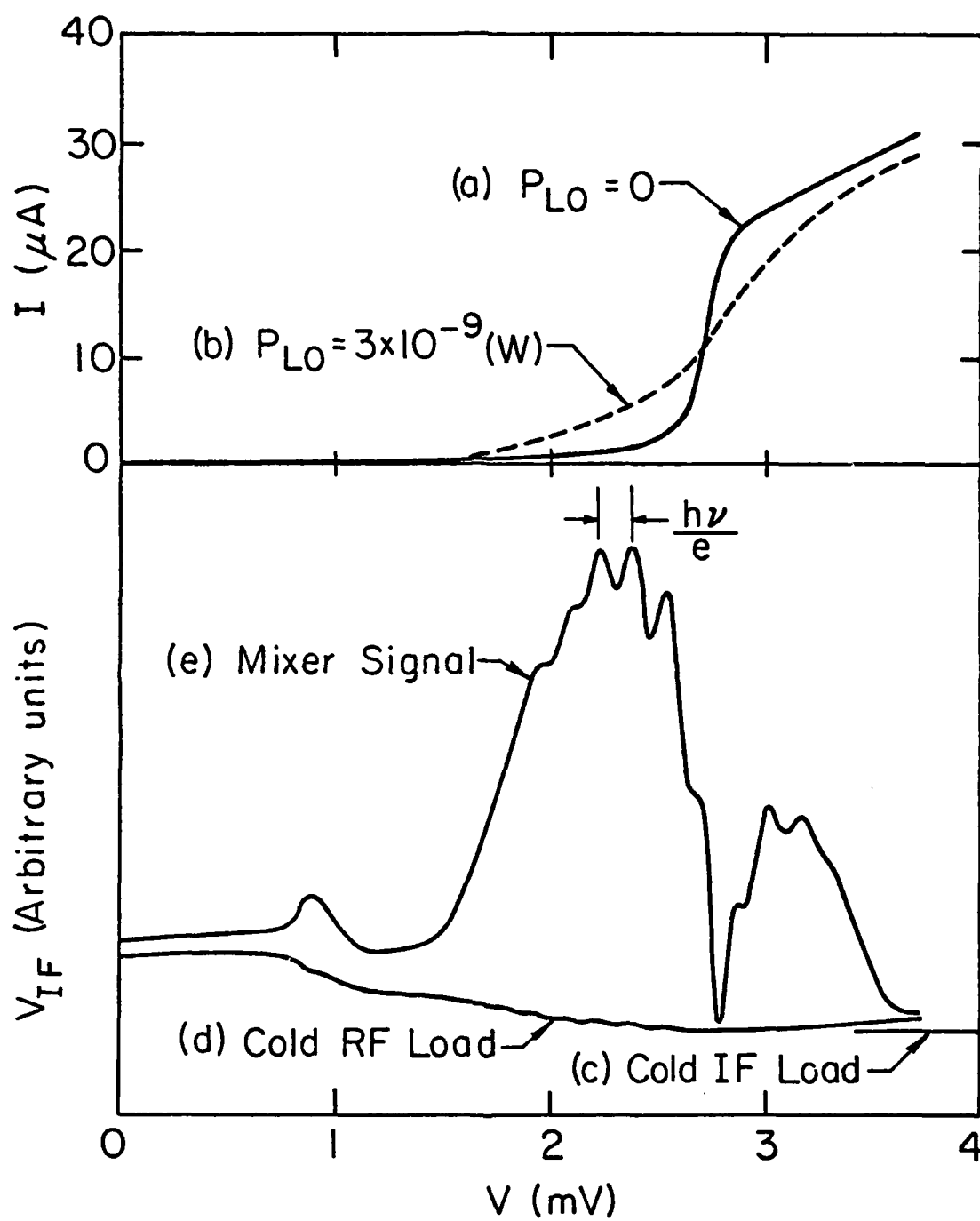


Figure 8.

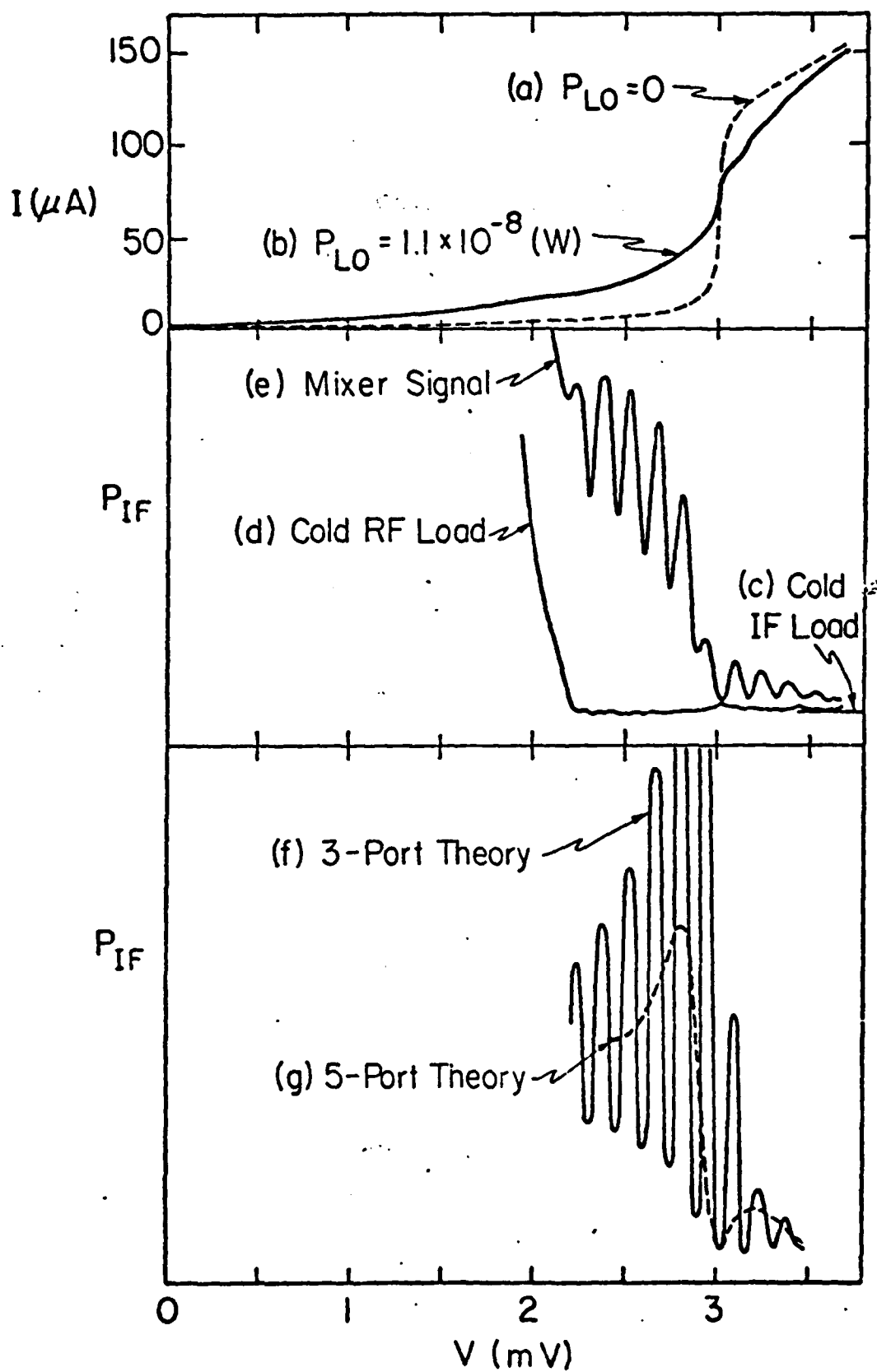


Figure 9.

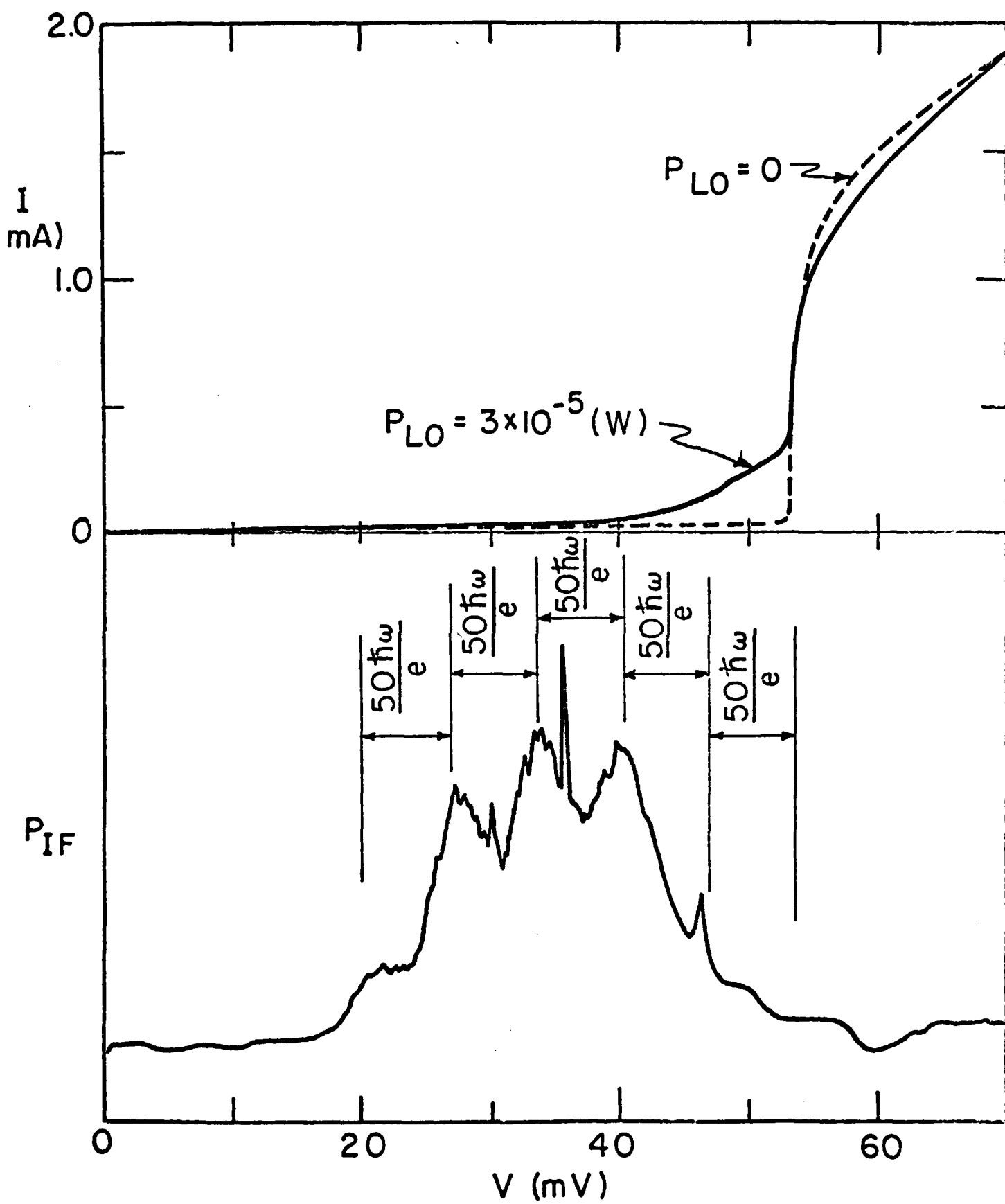


Figure 10.

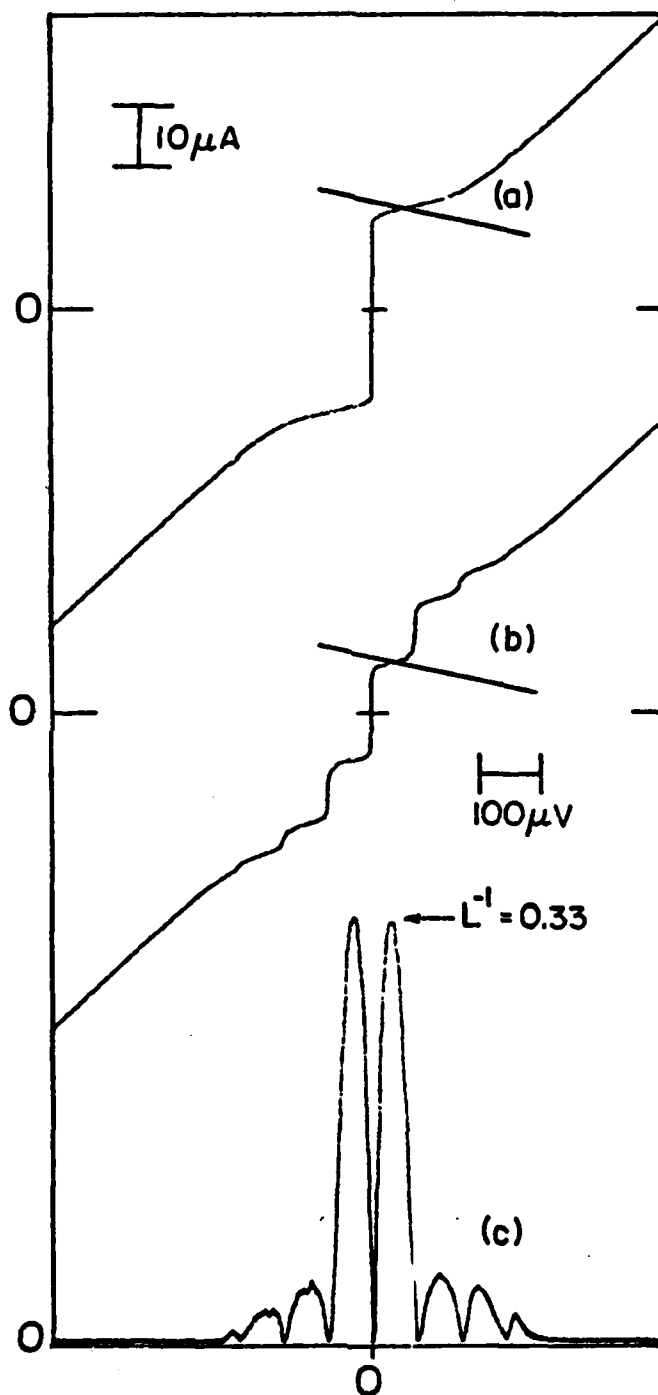


Figure 11.